HHS Public Access

Author manuscript

Cardiovasc Intervent Radiol. Author manuscript; available in PMC 2018 March 01.

Published in final edited form as:

Cardiovasc Intervent Radiol. 2017 March ; 40(3): 430–437. doi:10.1007/s00270-016-1515-y.

Cinnamic Acid Derivatives Enhance Efficacy of Transarterial Embolization in a Rat Model of Hepatocellular Carcinoma

Luke R. Wilkins, MD[1], **David L. Brautigan, PhD**[2], **Hanping Wu, MD, PhD**[3], **Hooman Yarmohammadi, MD**[4], **Ewa Kubicka, MS**[5], **Vlad Serbulea, BS**[6], **Norbert Leitinger, PhD**[7], **Wendy Liu, MD**[8], and **John R Haaga, MD**[9]

[1]Department of Radiology and Medical Imaging, University of Virginia Health Systems, Charlottesville, Virginia 22908

[2]Department of Microbiology, Immunology, and Cancer Biology, University of Virginia, Charlottesville, Virginia 22908

[3]Department of Radiology, University Hospitals of Cleveland, Case Western Reserve University, Cleveland, OH 44106

[4]Department of Radiology, Memorial Sloan-Kettering Cancer Center, New York, New York 10065

[5]Department of Microbiology, Immunology, and Cancer Biology, University of Virginia, Charlottesville, Virginia 22908

[6]Department of Pharmacology, University of Virginia, Charlottesville, Virginia 22908

[7]Department of Pharmacology, University of Virginia, Charlottesville, Virginia 22908

[8]Department of Pathology, University Hospitals of Cleveland, Case Western Reserve University, Cleveland, OH 44106

[9]Department of Radiology, University Hospitals of Cleveland, Case Western Reserve University, Cleveland, OH 44106

Abstract

Introduction—We hypothesize that combination of transarterial embolization (TAE) plus inhibition of lactate export will limit anaerobic metabolism and reduce tumor survival compared to TAE alone. The purpose of this study was to test this hypothesis in a rat model of HCC.

Methods—Rat N1-S1 hepatoma cells were assayed *in vitro* using the Seahorse XF analyzer to measure extracellular acidification (lactate excretion) comparing effects of addition of caffeic acid (CA) or ferulic acid (FA) or UK-5099 with control. Monocarboxylate transporter Slc16a3 was

CORRESPONDING AUTHOR: Luke R. Wilkins, MD, 1215 Lee Street, Box 800170, Charlottesville, Virginia 22908, Tel no. (434) 924-9279, Alternate Tel no. (517) 902-3328, Fax (434) 982-0887, correspondence (lrw6n@virginia.edu).

CONFLICTS

On behalf of all authors, the corresponding author states that there is no conflict of interest.

ETHICAL APPROVAL

All applicable institutional and/or national guidelines for the care and use of animals were followed.

INFORMED CONSENT

Does not apply.

knocked down by RNAi. N1S1 tumors were orthotopically implanted in rats and 4 groups evaluated: 1) Control, 2) TAE only, 3) TAE plus CA and 4) TAE plus FA. Tumor size was determined by ultrasound and analyzed by repeated measures statistics. Tumors harvested at 4 weeks were examined by microscopy.

Results—Seahorse assays showed that CA and FA caused significant reduction by >90% in lactate efflux by N1S1 tumor cells ($p<0.01$). Knockdown of Slc16a3 prevented inhibition by CA. *In vivo* tumors grew 30-fold in volume over 4 weeks in untreated controls. By comparison, TAE resulted in near cessation of growth (10% in 4 week time period). However, both TAE+CA and TAE+FA caused significant reduction of tumor volumes (87% and 72%, respectively) compared to control and TAE ($p<0.05$). Pathologic evaluation revealed residual tumor in the TAE group but no residual viable tumor cells in the TAE+CA and TAE+FA groups.

Conclusion—Addition of CA or FA enhances the effectiveness of TAE therapy for HCC in part by blocking lactate efflux.

Keywords

Tumor metabolism; interventional oncology; translational; lactate; embolization

INTRODUCTION

Hepatocellular carcinoma (HCC) is a relatively chemoresistant form of cancer (1, 2) with limited therapeutic options. Transarterial embolization (TAE) or transarterial chemoembolization (TACE) have been used extensively in non-surgical HCC patients with increased overall survival when compared to best supportive care. Despite advances and technical refinements, long-term survival of patients managed with TAE or TACE is not satisfactory, mainly as a result of the high rate of tumor recurrence, up to 70% (3). To improve clinical outcomes a different approach toward HCC treatment is warranted. Some authors question the superiority of TACE relative to TAE and there is evidence to suggest that the addition of chemotherapy does not contribute to the relative effectiveness of TACE in the treatment of HCC (4). The major tumoricidal mechanism in both TAE and TACE is thought to be the ischemic effect caused by occlusion of the arterial blood supply, blocking oxygen and nutrients that fuel tumor metabolism. Local recurrence of HCC following TACE may be from residual tumor that survives the procedure. One factor may be that although stasis is achieved based on angiography, there still remains substantial microvascular perfusion of the tumor (5). Regardless, reduced blood flow to the tumor due to embolization will impose limits on aerobic metabolism. We speculate the survival of residual tumors may occur through glycolytic metabolism.

Previous work has established that to maintain robust glycolysis, tumor cells need to efflux lactic acid to limit its buildup, which can exert inhibitory effects on glycolysis and cell growth (6). Lactate export from the cell is facilitated by a set of plasma membrane transporter proteins called monocarboxylate transporters (MCTs) (7, 8). Although 14 isoforms of MCTs have been identified in the human genome, only four of these (MCTs 1–4) are known to play a role in lactic acid transport in mammalian tissues, including tumors (9). Further, these MCT transporters have been identified in hepatocellular carcinoma cells,

making them a potential target for cancer therapy (6, 7). A group of compounds related to cinnamic acid (e.g. caffeic acid and ferulic acid) have been identified as potential inhibitors of MCT (8, 10). The aim of this study is to investigate the efficacy of two of these cinnamic acid derivatives (CAD) in N1-S1 hepatocellular carcinoma in a rat model.

MATERIALS AND METHODS

Analysis of N1-S1 cell metabolism *in vitro*

Rat hepatoma N1-S1 cells were purchased from ATCC (CRL-1604) and cultured in IMDM medium with 10% fetal bovine serum in dishes pre-coated with 1:10 dilution of polylysine (Sigma P8920). Cells were replated in polylysine coated XF-24 cell culture plates (1×10^5 cells/well in 500μl volume) for 12 hours. The XF sensor cartridge for the Extracellular Flux Analyzer (Seahorse Bioscience) was hydrated for 12 hours in a 37°C incubator without CO_2. For real-time analysis of the extracellular acidification rate (ECAR), cells were washed and then submerged in Glycolysis Stress Test Base Medium: DMEM D 5030 media base (Sigma-Aldrich), 2 mM L-glutamine (Gibco), and 143 mM NaCl, adjusted to pH 7.35 at 37°C as per the manufacturers' instructions. The Seahorse instrument measured ECAR in four separate wells in parallel for each treatment. Measurements of basal conditions were recorded at three successive times upon the start of the experiment. The test medium was then supplemented by injection of either vehicle (DMSO), or caffeic acid (final 1 mM), or ferulic acid (1 mM), or UK-5099 (100 μM), or no addition (control). These treatments remained throughout the remainder of the assay. Glycolysis was further stimulated by injection of glucose (Sigma) to a final concentration of 20 mM and ECAR measured at three time points. Later, oligomycin was added (at 1 μM) to block mitochondrial respiration and induce maximal glycolytic metabolism. At the final stage of the assay glycolysis was inhibited by addition of 80 mM 2-deoxy-D-glucose (Sigma). The net ECAR in response to 20 mM glucose were determined by subtracting the average ECAR level after 2-deoxy-D-glucose injection from the average ECAR level in 20 mM glucose.

Knockdown of the monocarboxylate transporter 4 (MCT4 a.k.a. Slc16a3) in N1-S1 cells used the rat SMART pool siRNA (Dharmacon, 0.04 uM) and transfection with Lipofectamine RNAiMax reagent (Invitrogen) for 6 hr in OptiMEM, then cells were rinsed and IMDM plus FBS added. In parallel, as control samples siRNA for luciferase (GL2, Invitrogen, 0.1 uM) was transfected into N1-S1 cells. Transfections were repeated after 24 hr, an approach we have used to maximize the extent of knockdown by siRNA. Cells were replated after an additional 24 hr into XF-24 assay plates and used the following day for assay, as described above. Western blotting with a commercial Slc16a3 antibody revealed multiple non-specific bands, so the extent of knockdown could not be estimated.

Rat syngeneic *in vivo* HCC tumor model

All procedures were in compliance with the National Institutes of Health Guide for the Care and Use of Laboratory Animals. Approval of the Institutional Animal Care and Use Committee was obtained before the study was initiated. For all surgical and imaging procedures, the animals were anesthetized with isoflurane 2–5% given by mask, to effect. The animals were monitored throughout the procedures and during recovery after each

procedure. Analgesia after surgery was administered as needed for pain with buprenorphine (0.01–0.05 mg/kg subcutaneously) every 8–12 hours. Euthanasia was performed by asphyxiation with carbon dioxide.

Rat N1-S1 cells were cultured in Iscove's modified Dulbecco's Medium (Catalog No. 30-2005, ATCC) with 5% fetal bovine serum and maintained at 37ºC and 5% CO_2 with passage biweekly. To establish liver tumors, 5×10^6 viable cells suspended in 0.2 ml medium without added serum were inoculated under the capsule of the medial aspect of the left lobe of the liver of male Sprague-Dawley rats (6 weeks old, Charles River, average weight, 200–250 g) after a mini-laparotomy. Tumors were allowed to grow for 14 days after implantation and ultrasound (US) evaluation was performed to evaluate tumor size.

For TAE therapy, after anesthesia was established, the upper abdomen was shaved and cleaned with iodine solution. Sterile towels were applied and intravenous access established. A 2 cm midline laparotomy was performed. The gastroduodenal artery was dissected under a stereomicroscope and cannulated retrograde with PE-50 polyethylene tubing. The common hepatic artery was temporarily occluded using a clip. The animals were divided into 4 separate treatment groups: 1) Control- 1 mL normal saline injection (NS) (n=5), 2) TAE done with polyvinyl alcohol (PVA) particles (10 mg 50–150 um diameter) in 1 mL NS (n=4), 3) TAE with PVA + 30 mg FA (ferulic acid) in 1 mL NS (n=5), 4) TAE with PVA + 30 mg CA (caffeic acid) in 1 mL NS (n=5). Doses of FA and CA were determined based on a review of the literature (11, 12) and our preliminary data. The TAE was done by slow injection over the course of 1 minute. The catheter tubing was removed and the gastroduodenal artery (GDA) was ligated. The abdominal wall was closed and the animals allowed to recover from anesthesia. Pre- and post-treatment contrast-enhanced ultrasound (CE-US) (Toshiba Aplio® SSA-770A) was performed to verify efficacy of embolization, evidenced by complete cessation of tumor blood flow, using a previously established technique (13). Tumor volume was determined by US twice a week for the next 4 weeks, pending survival. After 4 weeks the animals were euthanized and the tumors were dissected and histopathogic analysis was performed.

For tumor volume measurements, tumor length (L), width (W), and height (H) were measured by 2D-ultrasound. Tumor volume (V) was calculated by the formula: $V = 0.5 \times L \times W \times H$. Relative volume after treatment was calculated as the percentage of pre-treatment tumor volume. For pathologic analysis, non-tumorous liver tissue and tumor tissues were sliced at 2-mm intervals for gross examination, fixed in 10% formalin, and then stained with H&E. Tumor viability was estimated by light microscopic examination. The non-tumor liver tissue was evaluated for adverse effects of treatment. Histopathologic evaluation was performed by an independent pathologist (WL) who was blinded to which groups were being examined.

Tumor sizes (comparison to T0=100) were analyzed and compared between the treatment groups. Repeated measures models were used to analyze in vivo tumor growth over the 4 study weeks. Tumor volumes were transformed to the log scale, both to stabilize the variance and to facilitate the interpretation of growth in terms of fold changes. A power model was used for the within-animal correlations, allowing for exponentially decreasing

correlations as a function of the amount of time between measurements. F-tests based on contrasts were used to make specific comparisons among groups. Proper random multiple imputation (14), with 50 completed data sets, was used to check the effect of animal deaths prior to 28 days on the conclusions of the analysis. Analyses were carried out in SAS 9.4 PROC MIXED (Cary, NC).

RESULTS

Effects of caffeic acid or ferulic acid on N1-S1 cells *in vitro*

The rat hepatoma N1-S1 cell line was used in a Seahorse XF analyzer to assay for extracellular acidification rate (ECAR) as a measure of lactate excretion. In separate independent experiments (Figure 1) four samples were assayed in parallel under each condition, as technical replicates. Although the initial and peak ECAR values differed between the biological replicate experiments (Figure 1, parts A vs B), the responses to all treatments were faithfully reproduced. After recording basal ECAR for 20 min in all 20 samples one group remained untreated, to compare to groups with added vehicle (DMSO), or caffeic acid (CA), or ferulic acid (FA), or UK-5099. UK-5099 is known as an inhibitor of the mitochondrial pyruvate transporter and inhibits pyruvate-dependent O_2 consumption (15). In addition, UK-5099 is reportedly an inhibitor of MCTs and therefore provided a comparison to CA and FA. The untreated control and vehicle treated samples showed a stable level of ECAR, in contrast to samples treated with either CA or FA, where there was a steep time-dependent decline in ECAR to near zero at 30 min after addition representing >90% inhibition. We concluded that CA or FA effectively inhibited lactate export from N1-S1 cells. Addition of UK-5099 resulted in approximately a 20% decrease in ECAR during this same time period. At 50 min bolus addition of glucose (to 20 mM) to stimulate glycolysis elicited almost a 2-fold increase in ECAR in the controls, however ECAR was decreased by relatively 60–70% in cells exposed to either CA or FA, differences that were highly significant compared to vehicle control (Figure 1, part C, $p< 0.01$ and $p< 0.001$, and Figure 1, part D, $p< 0.0001$). Samples treated with UK-5099 plus glucose challenge had slightly reduced ECAR compared to control that bordered on statistical significance, with one experiment (Figure 1, part D) showing $p< 0.05$. Addition of oligomycin (at 80 min) to block aerobic respiration exposed the maximal glycolytic capacity of the cells. This capacity was reduced to the same extent, by approximately 50%, in response to any of the three agents, caffeic acid, ferulic acid or UK-5099. Finally, at 110 min addition of excess 2-deoxyglucose, which is not metabolized and interferes with glucose metabolism, suppressed ECAR in all samples, showing that ECAR was dependent on glycolysis. The oxygen consumption rate was measured by Seahorse and addition of either CA or FA resulted in about a 50% reduction. The reduced level was not changed following addition of glucose and was reduced to baseline by addition of oligomycin (not shown).

To test whether the action of CA was due to inhibition of lactate export we used RNAi to knockdown the expression of Slc16a3 (MCT4) in rat N1-S1 cells. As seen in Figure 2 there was > 90% inhibition of ECAR by added CA in control knockdown cells prior to a glucose challenge, and > 50% inhibition following the glucose challenge. This response was similar to that seen with untransfected N1-S1 cells (compare Figure 1A, 1B and Figure 2). The

inhibition by added CA was essentially eliminated in N1-S1 cells knocked down for MCT4 (Figure 2, closed squares vs. open circles). The Slc16a3 knockdown cells had ECAR values similar to the control cells, suggesting that other transporters in addition to MCT4 contributed to ECAR in these knockdown cells.

TAE treatments of orthotopic N1-S1 HCC in rats

Rat N1-S1 cells were orthotopically implanted in Sprague-Dawley rats and prior to start of treatments there was no statistically significant difference in tumor sizes. Following embolization, there was continuous, aggressive tumor growth observed in the control untreated group. During the course of observation due to tumor burden and anorexia three animals needed to be euthanized before the end of the schedule (2 on day 14 and 1 on day 24). In the two surviving animals tumor size increased greater than 3000 % from initial implantation. Tumor size was monitored by ultrasound with representative images provided in Figure 3.

All TAE treatments resulted in highly significant ($p < 0.0001$) reduction in tumor volume relative to the untreated control group. Relative tumor volumes for all treatment groups are plotted in Figure 4. Tumors treated with bland TAE (saline, as control) demonstrated about 10 % increase in size over the observation period (Figure 4, closed triangles). This represented a significant reduction ($p<0.001$) relative to untreated control tumors. One of the tumors in this TAE treatment group demonstrated continuous growth, whereas the other tumors increased in volume only at early observation times, and then later decreased in size. By comparison, TAE in combination with either of the CADs induced regression of the tumors, with 70–85% reduction in volume (note the logarithmic scale in Figure 4). The TAE +FA group showed decreased tumor volumes in all animals within the first week, and progressive reduction over the observation period (Figure 4, closed squares). These tumors measured an average of only 28% of their original size after the 4 weeks (Figure 4). The TAE+CA group demonstrated even more extensive reduction in tumor volumes in all animals, shrinking to only 13% of their original size at the end of the observation period (Figure 4, closed diamonds). The reduction in tumor volumes in the TAE+FA and TAE+CA groups both were statistically significant when compared to the TAE only group ($p < 0.05$). The results for TAE+CA and TAE+FA were not statistically significantly different from one another ($p = 0.14$), indicating that these compounds exerted similar effects on the tumors. In the three treatment groups (TAE, TAE+CA, and TAE+FA) there were no significant adverse events in any animals during the 4 week observation period.

Histopathologic evaluation of the specimens from control (Figure 5A) showed areas of tumor cells and some necrosis, compared to livers from the group treated with TAE that had significant areas of residual tumor (Figure 5B). On the other hand, histopathologic evaluation of the TAE+CA group showed extensive necrosis and no evidence of residual tumor (Figure 5C). Further, analysis of the adjacent liver parenchyma demonstrated minimal inflammatory changes and no evidence of bile duct proliferation or multinucleated giant cell reaction.

DISCUSSION

The present study was designed to evaluate the efficacy of two cinnamic acid derivatives (caffeic acid and ferulic acid) in an N1S1 model of HCC in Sprague-Dawley rats. Clinical research and experience has shown that response rates to TAE or TACE in HCC vary dramatically (1, 2, 4). HCC that survives these procedures may use both oxidative phosphorylation and anaerobic glycolysis (16). Glycolytic metabolism has been suggested as the preferred pathway for cancer cells (17, 18), and is well-known as the Warburg effect (19). Lactate is able to modulate pro-cancerous processes, for example increase the expression of vascular growth factors for vasculogenesis. However, if intracellular lactate levels become highly elevated, it provides a negative feedback loop on glycolysis and growth arrest because low pH inhibits glycolysis via the rate-limiting enzyme phosphofructokinase (20–24). To sustain growth and proliferation, cancer cells need to excrete lactate, for removal by lymphatics and veins (25–27). This export involves a family of monocarboxylate transporter (MCT) proteins with MCT4 prominently expressed in liver.

Our concept was to employ caffeic acid (CA) and ferulic acid (FA) that are considered relatively safe compounds and known to inhibit lactate export via the MCT4 transporter (9, 10). The expectation was that these compounds would result in elevated levels of intracellular lactate in hepatoma cells, providing a negative feedback on glycolysis, with inhibition of tumor growth. Indeed, *in vitro* assays showed that the CA and FA effectively blocked ECAR, as a measure of lactate export from N1-S1 cells during a glucose challenge. Knockdown of MCT4 rendered the ECAR by N1-S1 cells essentially resistant to inhibition by CA, confirming that MCT4 was required for this response. Overall, these results show that N1-S1 cells have a substantial capacity for glycolysis, and their export of lactate, in particular MCT4, is effectively inhibited by CA and FA.

The combination of TAE with CA or FA was associated with a 70–85% reduction of *in vivo* tumor burden when compared with TAE using embolic agent alone. Such an extensive reduction in tumor volume was unanticipated. The concentration of CA or FA achieved locally during the TAE procedure is likely higher than those tested *in vitro*. This is based on the concentration of the infused solution, and our estimates of the intravascular volume that was infused. Thus, the extent of MCT inhibition was likely as much *in vivo* as was seen in the *in vitro* experiments. The CA and FA reduced the viability of N1-S1 cells in culture (not shown), and it is possible this involves actions in addition to inhibition of MCT4. As phenolic compounds CA and FA have a more complex pharmacology that might contribute to their anti-tumor and anti-inflammatory actions. Phenolic compounds, specifically CA, have been found to generate reactive oxygen species (ROS) to create DNA fragmentation and apoptotic cell death in cancer cells (28). In addition, CA promotes cancer cell death through alterations in mitochondrial membrane potential and lipid peroxidation (28). These actions may contribute to the anti-tumorigenic effects when CA was administered in conjunction with TAE. Decreased peri-tumoral imflammation would be a beneficial effect in the clinic and could decrease post-procedure pain and levels of hepatic toxicity.

Potential limitations of this study include the nature of the tumor model. While the N1-S1 tumor model is a true rat hepatoma model, it is implanted within an otherwise normal liver

and is not subject to the same treatment challenges encountered in clinical practice when working with diseased hepatic parenchyma. Additionally, the embolization was not performed under direct fluoroscopic evaluation and was done via a catheterization of the GDA with temporary clamping of the common hepatic artery. While this method has been described previously and CE-US was used to confirm complete stasis following embolization, the overall procedure does not accurately reflect clinical practice. Further, we evaluated tumors based on volume, and the absolute volume measurements varied widely within a group. With a small number of animals in each group, this may have contributed to what appears as a large standard deviation. However, we evaluated the growth rates by repeated measures, comparing each tumor to itself over time, a statistically valid approach. Lastly, while promising, the results were not tested long-term and further research would be required to assess longer-term durability of the responses and if there is a survival benefit.

This study has implications for our current understanding of HCC and for future tumor treatments. Catheter-based oncologic therapies have long relied on inhibition of tumor growth via restricted blood supply, using embolic material. Metabolism has been considered as a target for oncologic treatment and here we have demonstrated the utility of this approach in HCC using this model system. The marked changes in tumor size, residual tumor, and peri-tumoral inflammatory changes we observed highlight the promise of using CA or FA as agents in conjunction with TAE. Further investigation into these pharmacologic agents is warranted to more accurately define the optimal delivery method, dose-response relationship, and long-term outcomes.

Acknowledgments

The authors wish to thank Mark Conway, PhD for his statistical analysis.

FINANCIAL SUPPORT

The research presented in this manuscript was supported by the Thelma R. Swortzel Collaborative Research Grant from the University of Virginia, the Paul Mellon Institute of the University of Virginia, and a grant from the NCI, NIH

References

1. Burroughs A, Hochhauser D, Meyer T. Systemic treatment and liver transplantation for hepatocellular carcinoma: two ends of the therapeutic spectrum. Lancet Oncol. 2004; 5:409–418. [PubMed: 15231247]
2. Asghar U, Meyer T. Are there opportunities for chemotherapy in the treatment of hepatocellular cancer? J Hepatol. 2012; 56:686–695. [PubMed: 21971559]
3. Miyayama S, Matsui O, Yamashiro M, Ryu Y, Kaito K, Ozaki K, et al. Ultraselective transcatheter arterial chemoembolization with a 2-f tip microcatheter for small hepatocellular carcinomas: relationship between local tumor recurrence and visualization of the portal vein with iodized oil. J Vasc Interv Radiol. 2007; 18:365–376. [PubMed: 17377182]
4. Marelli L, Stigliano R, Triantos C, Senzolo M, Cholongitas E, Davies N, et al. Transarterial therapy for hepatocellular carcinoma: which technique is more effective? A systematic review of cohort and randomized studies. Cardiovasc Intervent Radiol. 2007; 30:6–25. [PubMed: 17103105]
5. Johnson CG, Sharma KV, Levy EB, Woods DL, Morris AH, Bacher JD, et al. Microvascular perfusion changes following transarterial hepatic tumor embolization. J Vasc Interv Radiol. 2016; 27:133–41. [PubMed: 26321051]

6. Mathupala SP, Colen CB, Parajuli P, Sloan AE. Lactate and malignant tumors: a therapeutic target at the end stage of glycolysis. J Bioenerg Biomembr. 2007; 39(1):73–77. [PubMed: 17354062]
7. Kang KW, Jin MJ, Han HK. IGF-I receptor gene activation enhanced the expression of monocarboxylic acid transporter 1 in hepatocarcinoma cells. Biochem Biophys Res Commun. 2006; 342(4):1352–1355. [PubMed: 16516162]
8. Halestrap AP, Denton RM. Specific inhibition of pyruvate transport in rat liver mitochondria and human erythrocytes by a-cyano-4-hydroxycinnamate. Biochem J. 1974; 138:313–6. [PubMed: 4822737]
9. Halestrap AP, Meredith D. The Slc16 gene family—from monocarboxylate transporters (MCTs) to aromatic amino acid transporters and beyond. Pflugers Arch. 2004; 447:619–628. [PubMed: 12739169]
10. Spencer TL, Lehninger AL. L-lactate transport in ehrlich ascites-tumour cells. Biochem J. 1976; 154:405–14. [PubMed: 7237]
11. Wu YC, Hseih CL. Pharmacological effects of *Radix Angelica Sinesis* (*Danggui*) on cerebral infarction. Chin Med. 2011; 6:1–5. [PubMed: 21226952]
12. Gamaro GD, Suyenga E, Borsoi M, Lerman J, Pereira P, Ardenghi P. Effect of rosmarinic and caffeic acids on inflammatory and nociception process in rats. ISRN Pharmacol. 2011:1–6. ID 451682.
13. Krix M, Kiessling F, Vosseler S, Kiessline I, Le-Huu M, Fusenig NE, et al. Comparison of Intermittent-Bolus Contrast Imaging with conventional Power Doppler Sonography: Quantification of Tumor Perfusion in Small Animals. Ultrasound in Medicine and Biology. 2003; 29:1093–1103. [PubMed: 12946512]
14. Rubin, D. Multiple Imputation for Nonresponse in Surveys. New York: John Wiley and Sons; 1987.
15. Patterson JN, Cousteils K, Lou JW, Fox JEM, MacDonald PE, Joseph JW. Mitochondrial metabolism of pyruvate is essential for regulating glucose-stimulated insulin secretion. J Biol Chem. 2014; 289:13335–46. [PubMed: 24675076]
16. Nakasima RA, Paggi MG, Pedersen PL. Contributions of glycolysis and oxidative phosphorylation to adenosine 5′-triphosphate production in AS-30D hepatoma cells. Cancer Res. 1984; 44:5702–6.
17. Van Heiden MG. Understanding the Warburg Effect: The Metabolic Requirements of Cell Proliferation. Science. 2009; 324(5930):1029–1033. [PubMed: 19460998]
18. Weinberg, R. pRb and Control of the Cell Cycle Clock. In: Weinberg, R., editor. 2007 Biology of Cancer. New York: Garland Science; 2007. p. 255-306.
19. Alfarouk KO, Verduzco D, Rauch C, Muddathir AK, Adil HH, Elhassan GO, et al. Glycolysis, tumor metabolism, cancer growth and dissemination. A new pH-based etiopathogenic perspective and therapeutic approach to an old cancer question. Oncoscience. 2014; 1:777–802. [PubMed: 25621294]
20. Leite TC, Coelho RG, Da Silva D, Coelho WS, Marinho-Carvalho MM, Sola-Penna M. Lactate down regulates the glycolytic enzymes hexokinase and phosphofructokinase in diverse tissues from mice. FEBS Lett. 2011; 585(1):92–98. [PubMed: 21074528]
21. Lao MS, Toth D. Effects of Ammonium and Lactate on Growth and Metabolism of a Recombinant Chinese Hamster Ovary Cell Culture. Biotechnol Prog. 2008; 13(5):688–691.
22. Marx E, Mueller-Klieser W, Vaupel P. Lactate-induced inhibition of tumor cell proliferation. Int J Radiat Oncol Biol Phys. 1988; 14(5):947–955. [PubMed: 3360660]
23. Cruz HJ, Freitas CM, Alves PM, Moreira JL, Carrondo MJT. Effects of ammonia and lactate on growth, metabolism, and productivity of BHK cells. Enzyme Microb Technol. 2000; 27(1–2):43–52. [PubMed: 10862901]
24. Ozturk SS, Riley MR, Palsson BO. Effects of ammonia and lactate on hybridoma growth, metabolism, and antibody production. Biotechnol Bioeng. 1992; 39(4):418–431. [PubMed: 18600963]
25. Sattler UG, Meyer SS, Quennet V, Hoerner C, Knoerzer H, Fabian C, et al. Glycolytic metabolism and tumour response to fractionated irradiation. Radiother Oncol. 2010; 94(1):102–109. [PubMed: 20036432]

26. Quennet V, Yaromina A, Zips D, Rosner A. Tumor lactate content predicts for response to fractionated irradiation of human squamous cell carcinomas in nude mice. Radiother Oncol. 2006; 81(2):130–135. [PubMed: 16973228]

27. Haaga J, Haaga R. Acidic lactate sequentially induced lymphogenesis, phlebogenesis, and arteriogenesis (ALPHA) hypothesis: Lactate-triggered glycolytic vasculogenesis that occurs in normoxia or hypoxia and complements the traditional concept of hypoxia-based vasculogenesis. Surgery. 2013; 154:632–7. [PubMed: 23859305]

28. Prasad RN, Karthikeyan A, Karthikeyan S, Reddy BV. Inhibitory effect of caffeic acid on cancer cell proliferation by oxidative mechanism in human HT-1080 fibrosarcome cell line. Mol Cell Biochem. 2011; 349:11–19. [PubMed: 21116690]

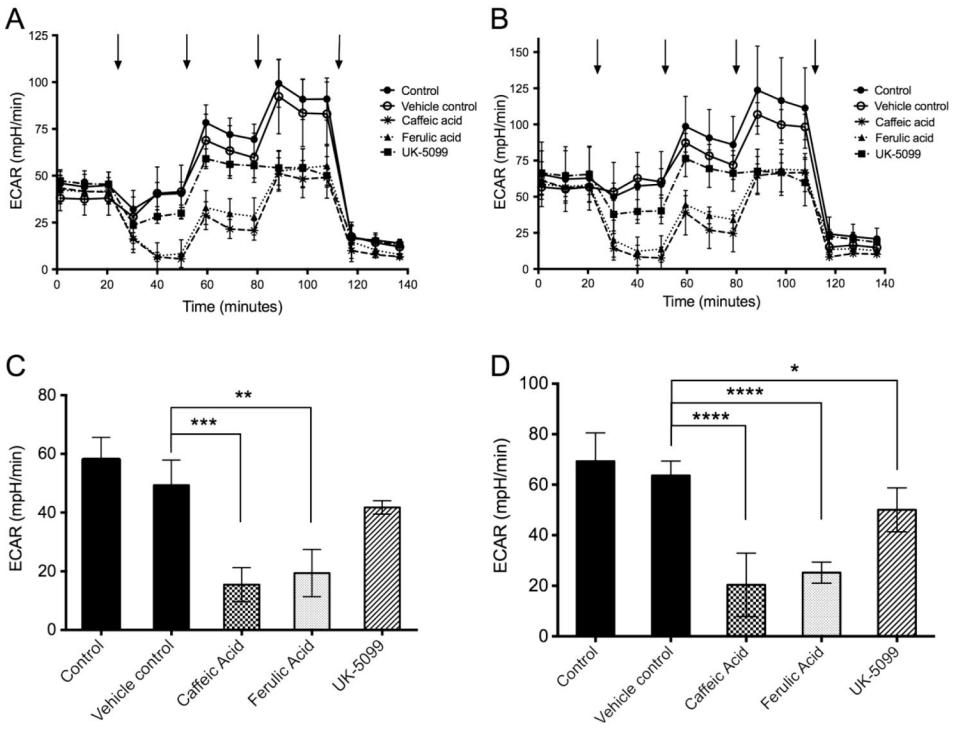

Figure 1.

Assay of N1-S1 rat hepatoma cells using Seahorse analyzer. Extracellular acidification rate (ECAR) was measured in parallel on four technical replicates for each condition (A), and average values plotted. The entire experiment was replicated independently (B), again with four samples in parallel for each condition. Untreated control, closed circles; vehicle (DMSO) treated, open circles; UK-5099, closed squares; ferulic acid, closed triangles; caffeic acid, astericks. The compounds or DMSO were added at 20 min and remained present throughout the remainder of the assay. Additions indicated by arrows at 50, 80 and 110 min were 20 mM glucose, 1 uM oligomycin, and 80 mM 2-deoxyglucose, respectively. The net ECAR under glucose challenge for each experiment (panels C and D, corresponding to A and B) was calculated from the difference between values with 20 mM glucose (50–80 min) and 80 mM deoxyglucose (120–140 min). * P,0.05, **, p<0.01, *** p< 0.001 and **** p< 0.0001.

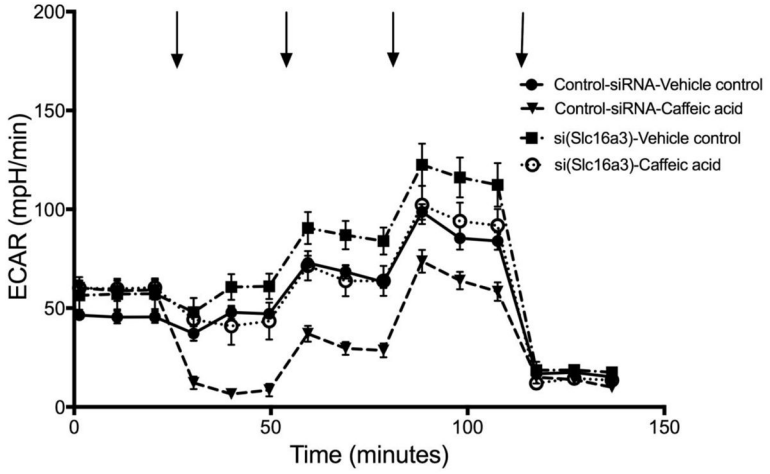

Figure 2.

Assay of N1-S1 rat hepatoma cells using Seahorse analyzer, comparing cells with control siRNA and knockdown of Slc16a3. Analysis of extracellular acidification rate (ECAR) was done in parallel on four technical replicates for each condition, as described for Figure 1. The entire experiment was replicated independently, again with four samples in parallel for each condition.

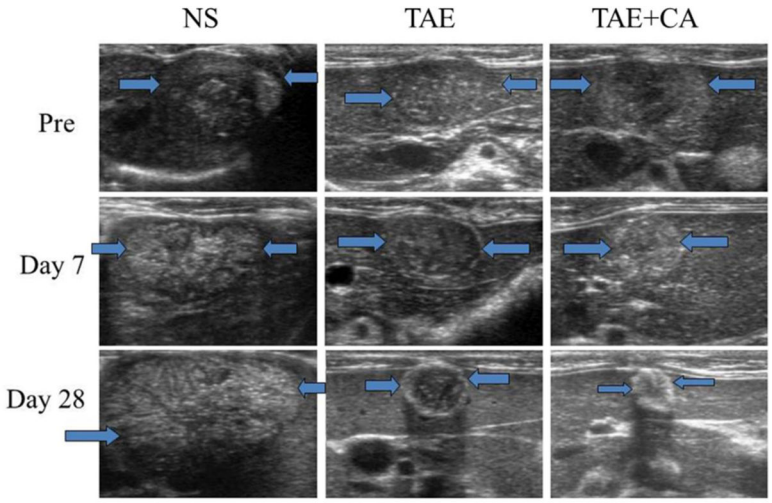

Figure 3.

Representative ultrasound (US) images of normal saline control group (NS), embolization only group (TAE), and embolization with caffeic acid group (TAE+CA) at day 0, 7, and 28. Note significant decrease in size of the TAE+CA group when compared with NS and TAE groups. TAE+FA groups showed similar decrease in size and changes in echogenicity when compared to TAE+CA.

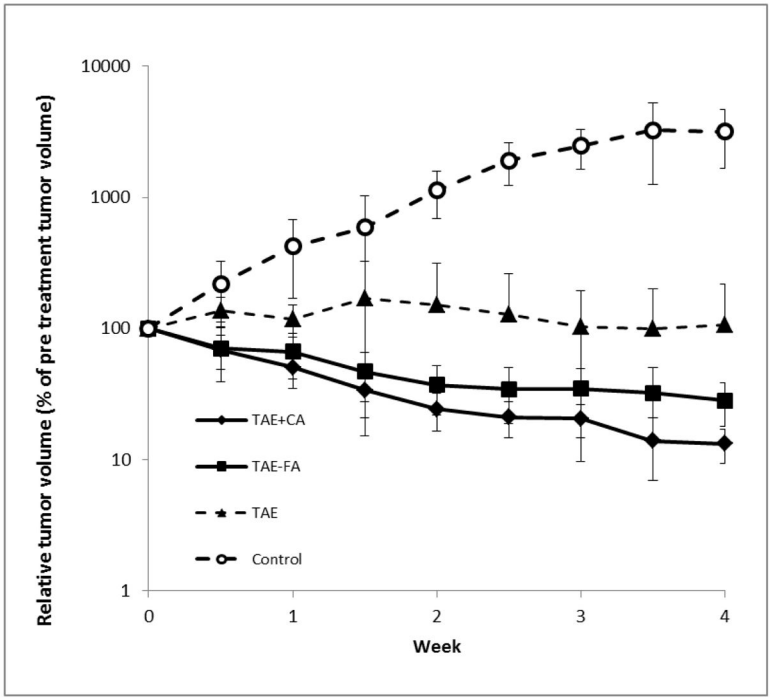

Figure 4.

Graph of logarithm of relative liver tumor volume determined by ultrasound vs. time in weeks. Groups TAE+CA and TAE+FA had n = 5 and TAE had n = 4 for the duration of the study. Control group started with n = 5 but due to tumor burden 2 animals were euthanized on day 14 and 1 animal on day 24. The average volumes in each group were calculated at each day of observation. Both TAE+CA and TAE+FA groups demonstrated a statistically highly significant ($p < 0.0001$) decrease in tumor size when compared to initial volumes in the same animals. Key to symbols is shown in Figure..

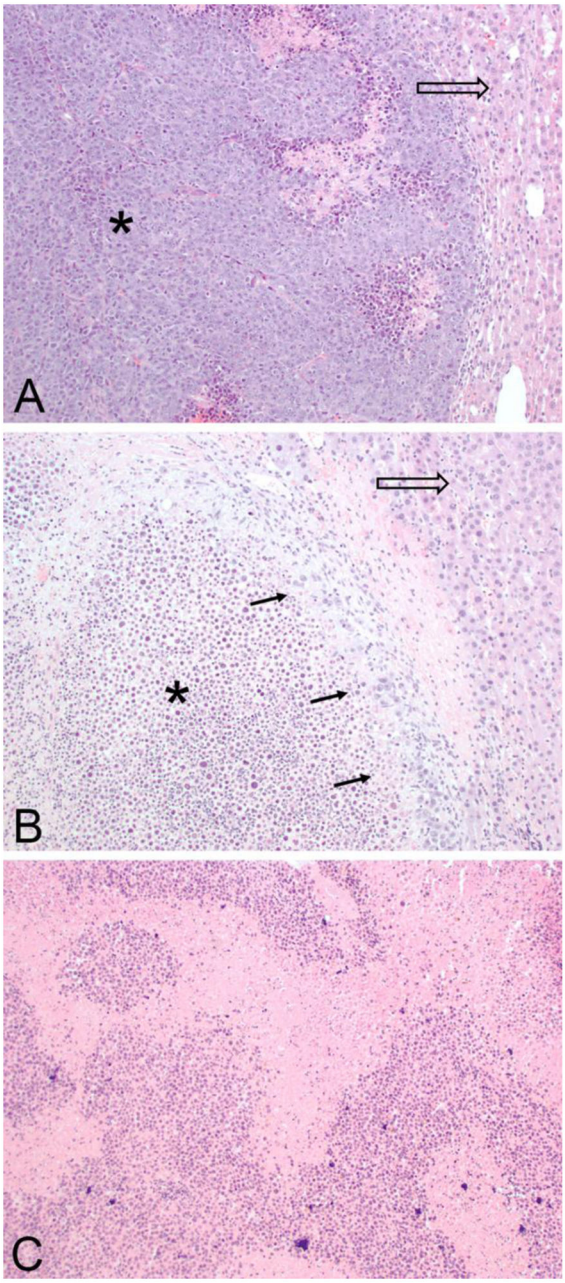

Figure 5.

Representative histopathologic microscopic images of livers. (A) A control specimen stained by H&E, imaged at 100x magnification showing extensive tumor (*) with necrosis and adjacent liver tissue (arrow). No peritumor inflammation or fibrosis noted. Surrounding liver shows no inflammatory changes or bile duct proliferation. (B) Specimen from embolization group (TAE) shows a majority of necrotic tumor (*) with rim of viable tumor cells (arrows) adjacent to normal liver (hollow arrow). No evidence of peritumor inflammation or bile duct proliferation. (C) Representative specimen from embolization with caffeic acid (TAE+CA)

shows entirely necrotic appearance of tumor area with no evidence of viable tumor. Background liver shows no inflammatory changes or bile duct proliferation (not imaged).